

# Faster Diffusion of Oxygen along Dislocations in (La,Sr)MnO<sub>3+δ</sub> Is a Space-Charge Phenomenon

Jacqueline M. Börgers, Joe Kler, Ke Ran, Elizabeth Larenz, Thomas E. Weirich, Regina Dittmann, Roger A. De Souza \*

J. M. Börgers

Institute of Physical Chemistry, RWTH Aachen University, 52056 Aachen, Germany

Peter Gruenberg Institute 7, Forschungszentrum Juelich GmbH, 52425 Juelich, Germany

J. Kler

Institute of Physical Chemistry, RWTH Aachen University, 52056 Aachen, Germany

Dr. K. Ran

Central Facility for Electron Microscopy, RWTH Aachen University, 52074 Aachen, Germany

E. Larenz

Institute of Physical Chemistry, RWTH Aachen University, 52056 Aachen, Germany

Prof. Dr. T. E. Weirich

Central Facility for Electron Microscopy, RWTH Aachen University, 52074 Aachen, Germany

Prof. Dr. R. Dittmann

Peter Gruenberg Institute 7, Forschungszentrum Juelich GmbH, 52425 Juelich, Germany

Prof. Dr. R. A. De Souza

Institute of Physical Chemistry, RWTH Aachen University, 52056 Aachen, Germany

Email Address: desouza@pc.rwth-aachen.de

## Supplementary Information

Grown La<sub>0.8</sub>Sr<sub>0.2</sub>MnO<sub>3</sub> thin films on SrTiO<sub>3</sub> were investigated by transmission electron microscopy. In Figure 1 obtained diffraction pattern taken along the [010] zone-axis of the thin film and the substrate are shown. For the film no splitting of diffraction spots in the pattern are observed, excluding the presence of any domains within the thin film.

For isotope exchange experiments the exact durations of equilibration and <sup>18</sup>O-isotope exchange are listed in Table 1. All obtained profiles are shown in Figure 2 for  $T = 600^\circ\text{C}$  and  $T = 625^\circ\text{C}$ ; in Figure 3 for  $T = 650^\circ\text{C}$  and in Figure 4 for  $T = 675^\circ\text{C}$  and  $T = 700^\circ\text{C}$ .

The isotope fraction  $n^*(x, t)$  is given by

$$n^*(x, t) = \frac{I_{18\text{O}}}{I_{18\text{O}} + I_{16\text{O}}}, \quad (1)$$

which ignores the presence of <sup>17</sup>O. The normalized isotope fraction  $n_r^*(x, t)$  is then obtained according to

$$n_r^*(x, t) = \frac{n^*(x, t) - n_{\text{bg}}}{n_g - n_{\text{bg}}}, \quad (2)$$

Table 1: Time  $t_{\text{pre-ex}}$  used for the pre-equilibration with <sup>16</sup>O and time  $t_{\text{ex}}$  used for <sup>18</sup>O exchange at temperatures  $T$ .

$T$ [°C]	$t_{\text{pre-ex}}$ [s]	$t_{\text{ex}}$ [s]
600	25800	6411 ± 63
625	25200	5329 ± 61
650	24725	5548 ± 63
675	20099	2791 ± 69
700	22684	1294 ± 59

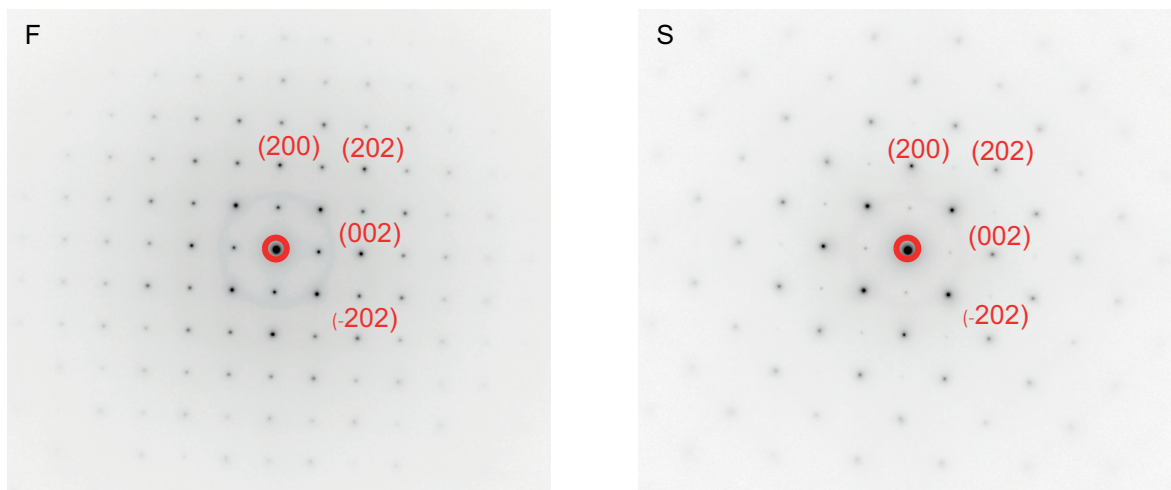


Figure 1: TEM diffraction pattern obtained for a 130 nm thick  $\text{La}_{0.8}\text{Sr}_{0.2}\text{MnO}_3$  thin films (marked as F, left pattern) on  $\text{SrTiO}_3$  (marked as S, right pattern). Labeling is based on the STO structure. Note that the halos visible in both patterns belong to the amorphous carbon used as capping layer and possible carbon contaminations.

where  $n_{\text{bg}}$  is the (natural isotopic) background level of  $^{18}\text{O}$  ( $\approx 0.2\%$ ) and  $n_{\text{g}}$  is the isotopic enrichment of gas used for exchange (that was here  $n_{\text{g}} = 78\%$ ).

In addition molecular dynamics (MD) simulations were performed using a simulation cell that was originally created for cubic  $\text{SrTiO}_3$  and adapted here first to  $\text{LaMnO}_3$  and, by substituting randomly 20% Sr, to  $\text{La}_{0.8}\text{Sr}_{0.2}\text{MnO}_3$ . Since  $\text{La}_{0.8}\text{Sr}_{0.2}\text{MnO}_3$  tends to undergo an orthorhombic transition we have examined the phase of the simulation cell by means of radial distribution function. In Figure 5 the distance of cations, namely Mn and La, is depicted, obtained within the bulk part of the simulation cell exemplary for  $T = 2000$  K. No deviation from the cubic phase was observed at any time during the simulations.

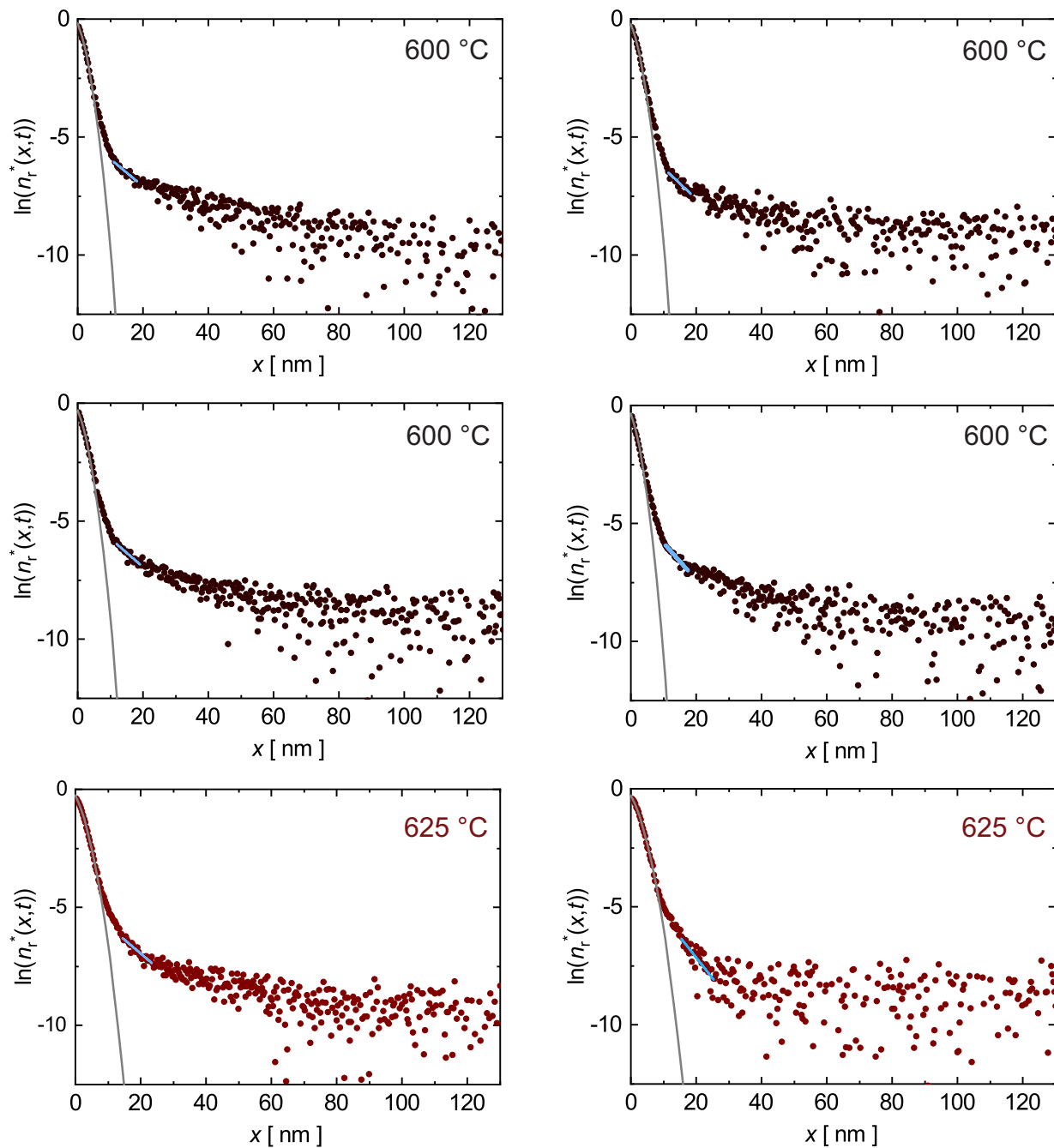


Figure 2:  $^{18}\text{O}$  diffusion profiles obtained for  $\text{La}_{0.8}\text{Sr}_{0.2}\text{MnO}_{3+\delta}$  by means of ToF-SIMS analysis shown as normalized isotope fraction  $n_r^*(x,t)$  versus depth  $x$  for  $T = 600^\circ\text{C}$  and  $T = 625^\circ\text{C}$ . Plotted are the fits to for the bulk (grey lines) and for the dislocation tails (blue lines).

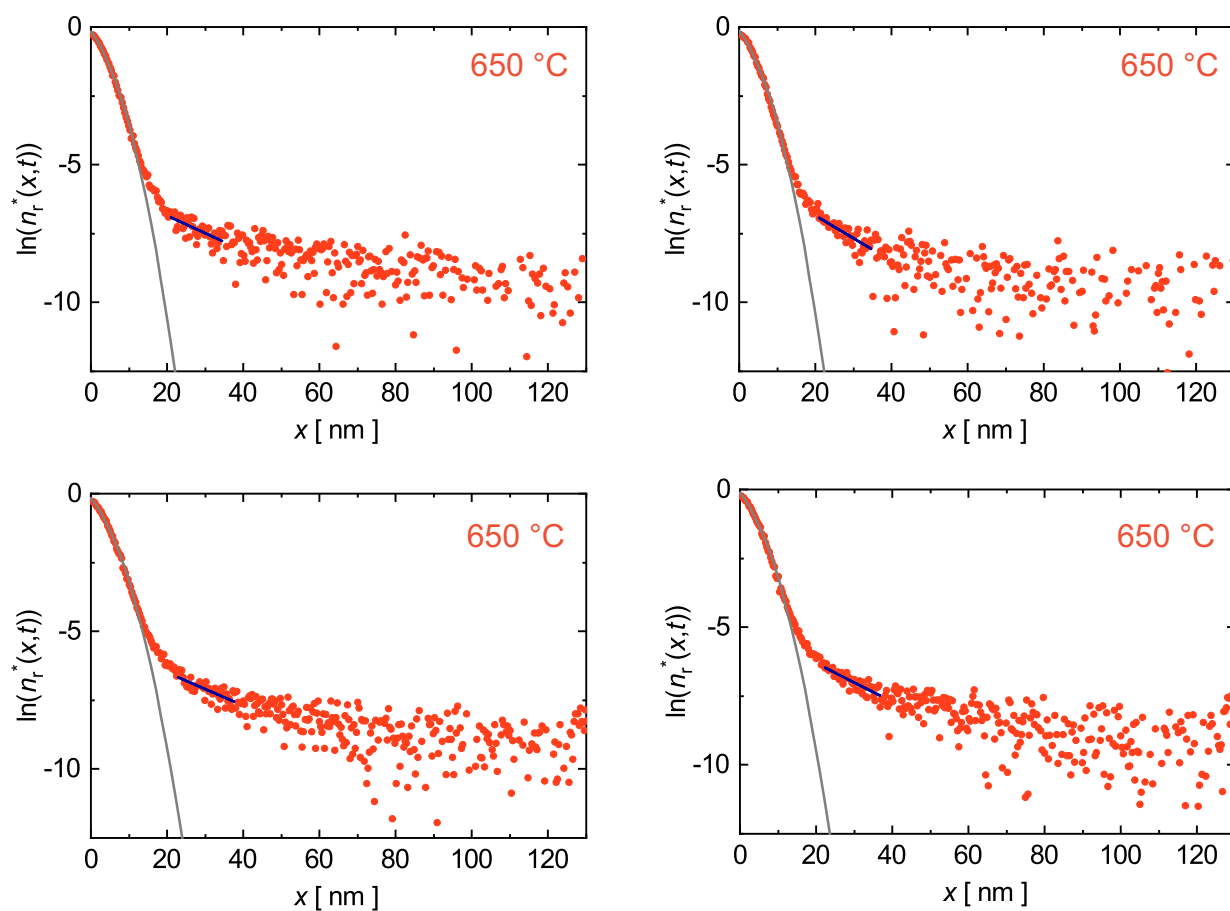


Figure 3:  $^{18}\text{O}$  diffusion profiles obtained for  $\text{La}_{0.8}\text{Sr}_{0.2}\text{MnO}_{3+\delta}$  by means of ToF-SIMS analysis shown as normalized isotope fraction  $n_r^*(x,t)$  versus depth  $x$  for  $T = 650^\circ\text{C}$ . Plotted are the fits to for the bulk (grey lines) and for the dislocation tails (dark blue lines).

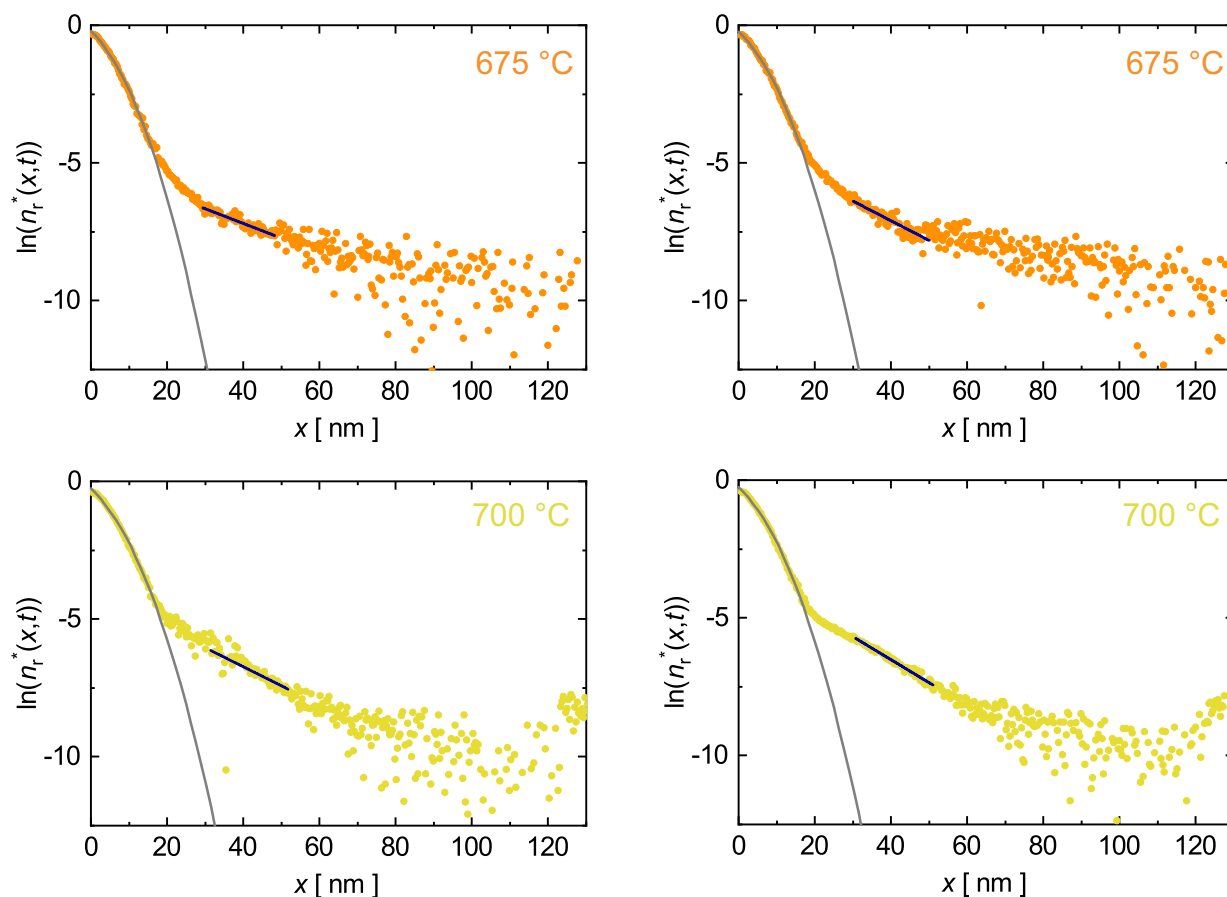


Figure 4:  $^{18}\text{O}$  diffusion profiles obtained for  $\text{La}_{0.8}\text{Sr}_{0.2}\text{MnO}_{3+\delta}$  by means of ToF-SIMS analysis shown as normalized isotope fraction  $n_r^*(x, t)$  versus depth  $x$  for  $T = 675^\circ\text{C}$  and  $T = 700^\circ\text{C}$ . Plotted are the fits to for the bulk (grey lines) and for the dislocation tails (dark blue lines).

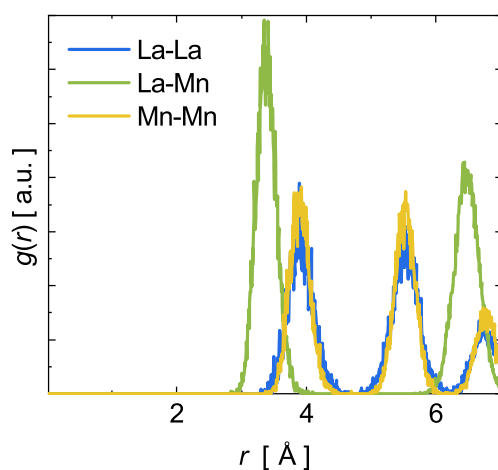


Figure 5: The separation of cations (Mn and La) are shown by means of the radial distribution function  $g(r)$  versus the distance  $r$ . The distance obtained for the cations shows a uniform separation according to the cubic lattice. The broadening of the peaks is due to thermal fluctuations, shown data are obtained at  $T = 2000\text{K}$ .